PROCEEDINGS OF SCIENCE

PDF and α_S constraints from jet measurements at CMS

Panagiotis KOKKAS[*†]
University of Ioannina
E-mail: pkokkas@uoi.gr

The measurements of the ratio of the inclusive 3-jet cross section to the inclusive 2-jet cross section, and of the double-differential cross section of 3-jet events are presented. The data sample was collected during 2011 at a proton-proton centre-of-mass energy of 7 TeV with the CMS detector at the LHC, corresponding to an integrated luminosity of 5.0 fb^{-1}. A comparison between the measurements and the predictions from perturbative QCD at next-to-leading order is performed. Within uncertainties, data and theory are in agreement. Both measurements are used for the extraction of the strong coupling constant, $\alpha_S(M_Z)$ with the results being in agreement with the world average value. The measurements also serve as a test of the evolution of the strong coupling constant at the 1 TeV region. No deviation from the expected behaviour is observed. The sensitivity of the observables to parameters of the theory like the parton distribution functions is also studied.

The European Physical Society Conference on High Energy Physics -EPS-HEP2013
18-24 July 2013
Stockholm, Sweden

[*]Speaker.
[†]For the CMS Collaboration.

PoS(EPS-HEP 2013)436

1. Introduction

Jet measurements at the LHC experiments are of great importance for several reasons: they provide a test of perturbative Quantum Chromodynamics (pQCD) in a previously unexplored energy region, and test the Standard Model (SM) predictions at high energy scales. They provide a precise measurement of the main background for many of the new physics searches. Jet measurements can also be used for the determination of the strong coupling constant, $\alpha_S(M_Z)$, test its running at high energy scales, and provide constraints on the parton density functions (PDF's).

In this proceedings, two new CMS measurements sensitive to $\alpha_S(M_Z)$ are reported. The ratio of the inclusive 3-jet cross section to the inclusive 2-jet cross section [1], and of the double-differential cross section of 3-jet events [2]. Both measurements are used for the extraction of the strong coupling constant. The data sample was collected during 2011 at a proton-proton centre-of-mass energy of 7 TeV with the CMS detector [3] at the LHC, corresponding to an integrated luminosity of 5.0 fb^{-1}.

2. The measurements

The ratio R_{32} of the inclusive 3-jet cross section to the inclusive 2-jet cross section [1] is proportional to $\alpha_S(Q)$ where Q is defined as the average transverse momentum of the two jets leading in p_{T},

$$Q = \langle p_{\mathrm{T}1,2} \rangle = \frac{p_{\mathrm{T}1} + p_{\mathrm{T}2}}{2}. \tag{2.1}$$

Many theoretical systematic uncertainties related to the choice of the renormalization and factorization scales, μ_r and μ_f, or to nonperturbative effects are reduced in the cross section ratio. In addition, experimental uncertainties such as those due to the jet energy scale largely cancel in the measurement of R_{32} . The uncertainty on the integrated luminosity measurement cancels completely. The ratio R_{32} also voids direct dependence on PDFs and the renormalization group equation (RGE) of QCD.

Figure 1 on the left shows the measurement of R_{32} and next-to-leading order (NLO) predictions using the NNPDF2.1-NNLO PDF set [4]. The upper panel of the plot shows the ratio R_{32} (solid circles) together with the NLO prediction (solid line) corrected for nonperturbative (NP) effects, the scale uncertainty, and the PDF uncertainty. At the bottom panel it is shown the ratio of data to the theoretical predictions, together with bands representing the scale (dotted lines) and PDF (solid lines) uncertainties. The error bars correspond to the total uncertainty. Within uncertainties the NNPDF2.1 PDF set is able to describe the data. The same stands also for theoretical predictions employing the MSTW2008 [5, 6], and CT10 [7] NNLO PDF sets.

At Figure 1 on the right it is shown the NLO predictions using the NNPDF2.1-NNLO PDF set for a series of values of $\alpha_S(M_Z)$, together with the measured R_{32} . The $\alpha_S(M_Z)$ value is varied in the range 0.106–0.124. The figure demonstrates the sensitivity of the ratio R_{32} to $\alpha_S(M_Z)$.

The value of $\alpha_S(M_Z)$ is determined by minimizing the χ^2 between the experimental measurement and the theoretical predictions. The result of the fit to the region of 420-1390 GeV is $\alpha_S(M_Z) = 0.1148 \pm 0.0014\,(\mathrm{exp.}) \pm 0.0018\,(\mathrm{PDF})\,^{+0.0050}_{-0.0000}\,(\mathrm{scale})$ with $\chi^2/N_{\mathrm{dof}} = 22.0/20$ at minimum. The experimental uncertainty contains the statistical, jet energy scale (JES), and unfold-

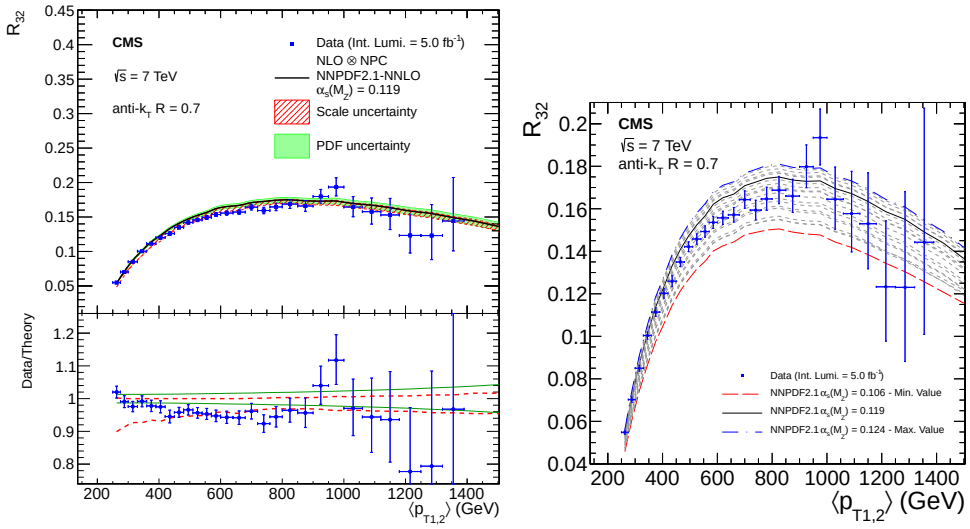

Figure 1: On the left the measurement of R_{32} and NLO predictions using the NNPDF2.1-NNLO PDF set. In the upper panel, the ratio R_{32} (solid circles) together with the NLO prediction (solid line) corrected for nonperturbative (NP) effects, the scale uncertainty, and the PDF uncertainty are shown. The bottom panel shows the ratio of data to the theoretical predictions, together with bands representing the scale (dotted lines) and PDF (solid lines) uncertainties. The error bars correspond to the total uncertainty. On the right, the NLO predictions using the NNPDF2.1-NNLO PDF set for a series of values of $\alpha_S(M_Z)$, together with the measured R_{32} . The $\alpha_S(M_Z)$ value is varied in the range 0.106–0.124.

ing sources, with the JES uncertainty being the dominant one. The measurement is dominated by the theoretical uncertainties and is in agreement with the world average value of $\alpha_S(M_Z) = 0.1184 \pm 0.0007$ [8].

The second measurement, reported in these proceedings, is the double-differential 3-jet mass cross section [2] as a function of the invariant mass m_3 and the maximum rapidity $y_{\max}$ of the 3-jet system with

$$m_3{}^2 = (p_1 + p_2 + p_3)^2 \tag{2.2}$$

$$y_{\max} = sign(|max(y_1,y_2,y_3)| - |min(y_1,y_2,y_3)|) \cdot max(|y_1|,|y_2|,|y_3|) \tag{2.3}$$

where p_i and y_i are the four-momentum and rapidity of the i-th jet leading in p_T. The measurement is done in two rapidity bins with $|y_{\max}| < 1$ and $1 \leq |y|_{\max} < 2$. For this observable the LO process is proportional to $\alpha_S{}^3$ and theory predictions are available up to NLO such that precise comparisons to data are possible. Constraints on the PDFs of the proton are studied and α_S is extracted from the $|y_{\max}| < 1$ bin, which exhibits the smallest experimental uncertainty.

Figure 2 presents the comparison of the unfolded 3-jet mass distribution to the NLO prediction employing the MSTW2008-NLO PDF set and multiplying by the NP correction factor. It is observed that pQCD is able to describe the 3-jet mass cross section over five orders of magnitude and for 3-jet masses up to 3 TeV. To better judge potential differences between data and theory, the ratios of the measured cross sections for the inner rapidity bin $|y|_{\max} < 1$ to the theory predictions

are presented in Fig. 3. Results are similar also for the outer rapidity bin $1 \leq |y|_{\max} < 2$. Within uncertainties most PDF sets are able to describe the data. Small deviations are visible with the HERAPDF1.5 NLO set [9]. Significant disagreements are exhibited by the ABM11 PDFs [10].

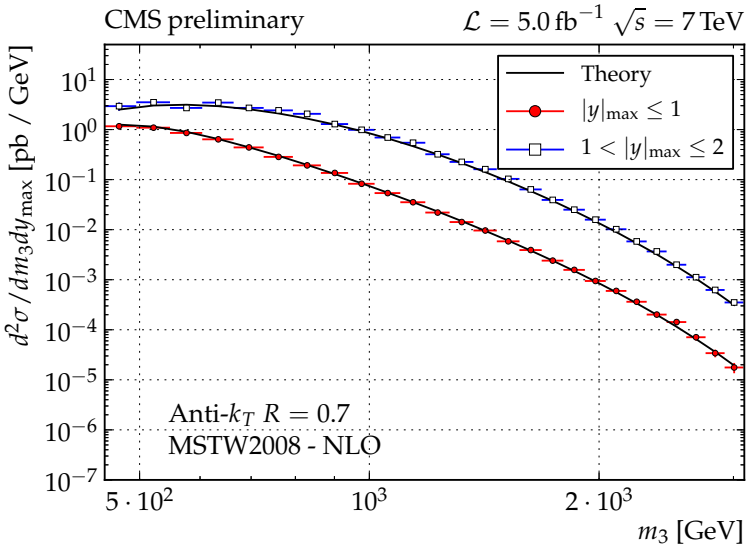

Figure 2: Comparison of the unfolded 3-jet mass cross section with the NLO prediction times NP corrections for the two considered regions in $|y|_{\max}$ using the MSTW2008-NLO PDF set. The error bars represent the total experimental uncertainty.

Concidering the PDFs as external input, the value of $\alpha_S(M_Z)$ can be determined by minimizing the χ^2 between the experimental measurement and the theoretical predictions. The result of the fit is $\alpha_S(M_Z) = 0.1160 \pm^{0.0025}_{0.0023} (\text{exp, PDF, NP}) \pm^{0.0068}_{0.0021} (\text{scale})$, with $\chi^2/N_{\text{dof}} = 9.11/26$ at minimum. The measurement is dominated by the theoretical uncertainties and is in agreement with the world average value [8].

To investigate the running of the strong coupling constant in more detail, the fitted region of the R_{32} and of the 3-jet mass cross section is split into three and eight bins, repectively, and the fitting procedure is repeated in each of these bins. The $\alpha_S(M_Z)$ determinations are then evolved back to the corresponding values $\alpha_S(Q)$ using the solution to the RGE.

Figure 4 shows the comparison of the $\alpha_S(Q)$ evolution as determined in the 3-jet mass cross section analysis from all measurement bins at central rapidity (curve with uncertainty band) to the world average (upper curve). The error bars on the data points correspond to the total uncertainty. The results from the R_{32} analysis [1] and a new CMS result from $t\bar{t}$ production [11] are also shown. In addition an overview of measurements of the running of the strong coupling constant $\alpha_S(Q)$ from electron-positron collider experiments [12, 13, 14], electron-proton experiments [15, 16, 17], and proton/anti-proton collider experiments [18, 19] is presented. All three CMS results are consistent with the evolution of the strong coupling as predicted by the renormalization group equation and with the world average on $\alpha_S(M_Z)$ and extend the covered range in scale Q up to the value of ≈ 1.4 TeV.

Data are also suitable to constrain the PDFs. To demonstrate this, Figure 5 presents the corre-

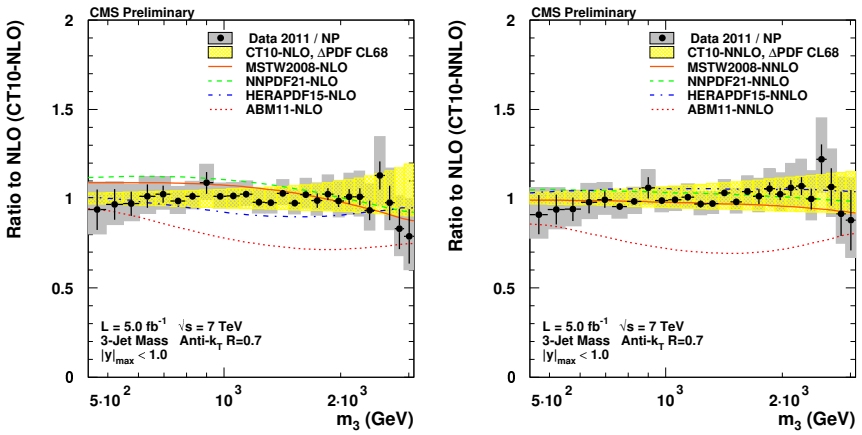

Figure 3: Ratio of the unfolded 3-jet mass distribution to the theory prediction including NP effects using PDF sets with NLO (left) or NNLO (right) PDF evolution in the inner rapidity bin $|y|_{\max} < 1$. The data are shown with error bars representing the statistical uncertainty and gray squares for the systematic uncertainties. The PDF uncertainty is shown for the CT10 PDF set at 68% confidence level as yellow band. In addition the central predictions are displayed for the other four examined PDF sets MSTW2008, NNPDF2.1, HERAPDF1.5, and ABM11.

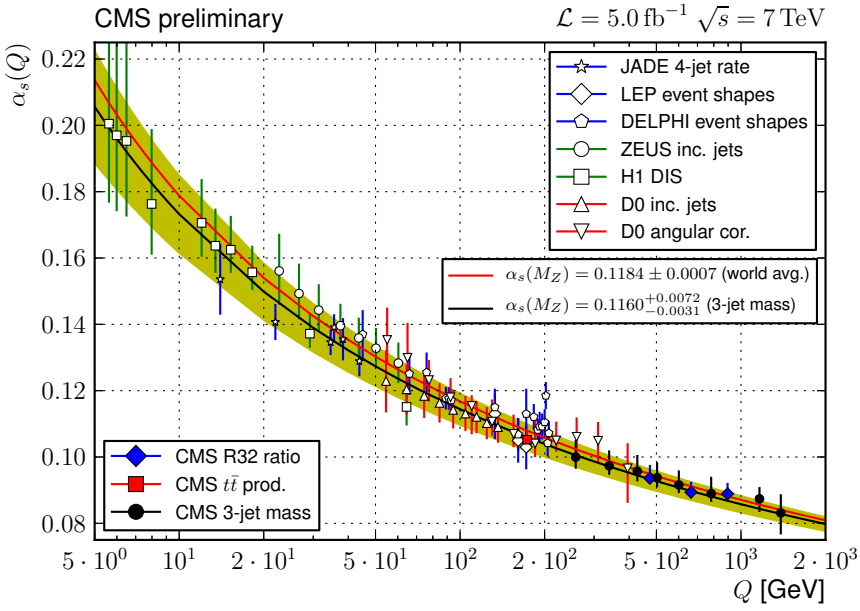

Figure 4: Comparison of the $\alpha_S(Q)$ evolution as determined in the 3-jet mass cross section analysis from all measurement bins at central rapidity (curve with uncertainty band) to the world average (upper curve). The error bars on the data points correspond to the total uncertainty. The CMS results from the R_{32} analysis [1] and from $t\bar{t}$ production [11] are also shown. In addition an overview of measurements of the running of the strong coupling constant $\alpha_S(Q)$ from electron-positron collider experiments [12, 13, 14], electron-proton experiments [15, 16, 17], and proton/anti-proton collider experiments [18, 19] is presented.

lation coefficient $\rho_i(x,Q^2)$ between the 3-jet mass cross section $\sigma_{m_3}(x,Q^2)$ and x times the parton distribution function $f_i(x,Q^2)$ as derived from the replicas of the NNPDF2.1 PDF set. The resulting correlation coefficients are shown for the up- and down-quark, and the gluon in the inner rapidity bin $|y|_{\max} < 1$, and demonstrate the potential impact at high x, in particular for the gluon between $0.05 < x < 0.5$. The correlations behave similarly in the outer rapidity bin.

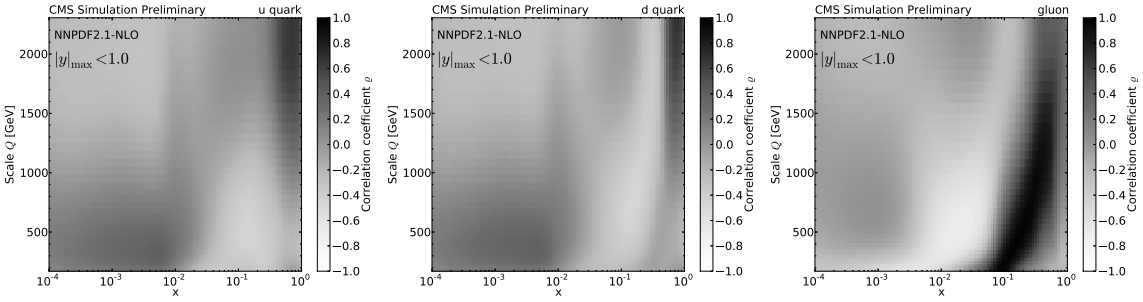

Figure 5: Correlation coefficient $\rho_i(x,Q^2)$ between the 3-jet mass cross section $\sigma_{m_3}(x,Q^2)$ and x times the parton distribution function $f_i(x,Q^2)$ as derived from the replicas of the NNPDF2.1 PDF set. The correlation is presented for the up (left), down (middle) and gluon (right) parton distributions in the inner rapidity bin $|y|_{\max} < 1$.

3. Conclusions

Two new CMS measurements sensitive to the strong coupling constant are reported, the ratio of the inclusive 3-jet cross section to the inclusive 2-jet cross section, and of the double-differential cross section of 3-jet events. Both measurements are used for the extraction of the strong coupling constant, with the results found to be in agreement with the world average value. Furthermore the two measurements serve as a test of the evolution of the strong coupling constant at the 1 TeV region, where no deviation from the expected behaviour is observed. It is also demonstrated that these data are suitable to constrain the PDFs.

4. Acknowledgments

This paper is Co-funded by the European Union (European Social Fund - ESF) and Greek national funds through the Operational Program "Education and Lifelong Learning" of the National Strategic Reference Framework (NSRF).

References

[1] CMS Collaboration, [hep-ex/1304.7498].

[2] CMS Collaboration, [CMS PAS SMP-12-027].

[3] CMS Collaboration, *JINST* **3** (2008) S08004.

[4] R. D. Ball et al., *Nucl. Phys. B* **849** (2011) 296.

[5] A. D. Martin et al., *Eur. Phys. J. C* **63** (2009) 189.

[6] A. D. Martin et al., *Eur. Phys. J. C* **64** (2009) 653.

[7] H.-L. Lai et al., *Phys. Rev. D* **82** (2010) 074024.

[8] Particle Data Group, *Phys. Rev. D* **86** (2012) 010001.

[9] H1 and ZEUS Collaboration, *JHEP* **109** (2010) 109.

[10] S. Alekhin et al., *Phys. Rev. D* **86** (2012) 054009.

[11] CMS Collaboration, [hep-ex/1307.1907].

[12] JADE Collaboration, *Eur. Phys. J. C* **48** (2006) 3.

[13] DELPHI Collaboration, *Eur. Phys. J. C* **37** (2004) 1.

[14] S. Marti i Garcia, [hep-ex/9704016].

[15] H1 Collaboration, *Eur. Phys. J. C* **65** (2010) 363.

[16] H1 Collaboration, *Eur. Phys. J. C* **67** (2010) 1.

[17] ZEUS Collaboration, *Nucl. Phys. B* **864** (2012) 1.

[18] D0 Collaboration, *Phys. Rev. D* **80** (2009) 111107.

[19] D0 Collaboration, *Phys. Lett. B* **718** (2012) 56.

PoS(EPS-HEP 2013)436